Electronic Supplemental Information (ESI)

Title

Two-Step Naked-Eye Detection of a Lectin by Hierarchical Organization of Soft Nanotubes into Liquid Crystal and Gel Phases

Authors

Naohiro Kameta,* Mitsutoshi Masuda, and Toshimi Shimizu

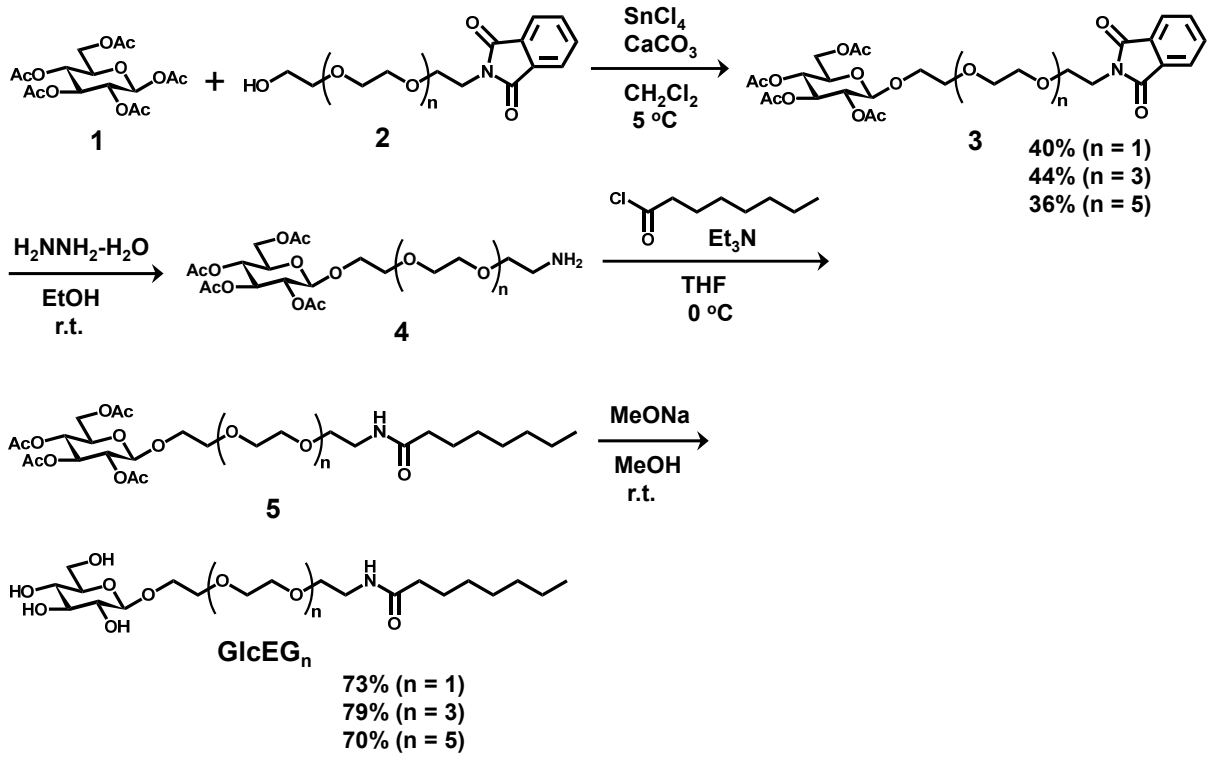

Scheme S1 Synthesis of **$GlcEG_1$**, **$GlcEG_2$**, and **$GlcEG_3$**.

The compound **2** was synthesized according to a following literature: D. Parker, *Macrocycle Synthesis*, Oxford University, 1996.
The glycosylation was carried out according to a following literature: T. Murakami et al., *Carbohydrate Research* 2007, **342**, 1009.

3 (n=3): 1H-NMR (400 MHz, in CDCl3), 7.85 (2H, *m*, phthalimide), 7.23 (2H, *m*, phthalimide), 5.31 (1H, *t*, GlcH-1), 5.26 (1H, *t*, GlcH-3), 5.06 (1H, *t*, GlcH-4), 4.92 (1H, *t*, GlcH-2), 4.31 (1H, *dd*, GlcH-6a), 4.07 (1H, *dd*, GlcH-6b), 3.90 (2H, *t*, -CH_2-), 3.84 (1H , *m*, Glc-H5), 3.75 (4H, *t*, -CH_2-), 3.60-3.67 (12H, *m*, -$(OCH_2CH_2O)_3$-), 3.26 (2H, *t*, -CH_2-), 2.07 (3H, *s*, Glc-OAc), 2.04 (3H, *s*, Glc-OAc), 2.03 (3H, *s*, Glc-OAc), 2.02 (3H, *s*, Glc-OAc). ESI-MS (m/z): 698.27 $[M + H]^+$.

3 (n=1): 1H-NMR (400 MHz, in CDCl3), 3.60-3.67 (4H, *m*, -OCH_2CH_2O-), the other data are similar to those of **3 (n=3)**. ESI-MS (m/z): 610.22 $[M + H]^+$.

3 (n=5): 1H-NMR (400 MHz, in CDCl3), 3.60-3.67 (20H, *m*, -$(OCH_2CH_2O)_5$-), the other data are similar to those of **3 (n=3)**. ESI-MS (m/z): 786.32 $[M + H]^+$.

GlcEG$_3$: 1H-NMR (400 MHz, in DMSO-d6), 7.75 (1H, *br*, NH), 4.96 (1H, *d*, GlcOH-4), 4.87 (1H, *d*, GlcOH-3), 4.81 (1H, *t*, GlcOH-2), 4.69 (1H, *t*, GlcH-1), 4.47 (1H, *t*, GlcOH-6), 3.63 (1H, *m*, GlcH-6a), 3.4 (1H, *m*, GlcH-6b, and 16H, *m*, –CH_2-(OCH_2CH_2O)$_3$-CH_2-), 3.1-2.9 (1H, GlcH-4; 3H, GlcH-2, -3, -5; 2H, Glc-O-CH_2-; 2H, -C*H$_2$*-NHCO-), 2.07 (2H, *m*, CO-CH_2-), 1.47 (2H, *m*, CO-CH_2-C*H$_2$*-), 1.23 (8H, *m*, -CH_2-), 0.85 (3H, *t*, -CH_3). Anal. calcd for $C_{24}H_{47}NO_{11}$: C 54.84, H 9.01, N 2.66. Found: C 54.75, H 9.09, N 2.58.

GlcEG$_1$: 1H-NMR (400 MHz, in DMSO-d6), 3.4 (1H, *m*, GlcH-6b, and 8H, *m*, –CH_2-OCH_2CH_2O-CH_2-), the other data are similar to those of **GlcEG$_3$**. Anal. calcd for $C_{20}H_{39}NO_9$: C 54.90, H 8.98, N 3.20. Found: C 54.80, H 9.08, N 3.10.

GlcEG$_5$: 1H-NMR (400 MHz, in DMSO-d6), 3.4 (1H, *m*, GlcH-6b, and 24H, *m*, –CH_2-(OCH_2CH_2O)$_5$-CH_2-), the other data are similar to those of **GlcEG$_3$**. Anal. calcd for $C_{28}H_{55}NO_{13}$: C 54.80, H 9.03, N 2.28. Found: C 53.72, H 10.02, N 2.13.

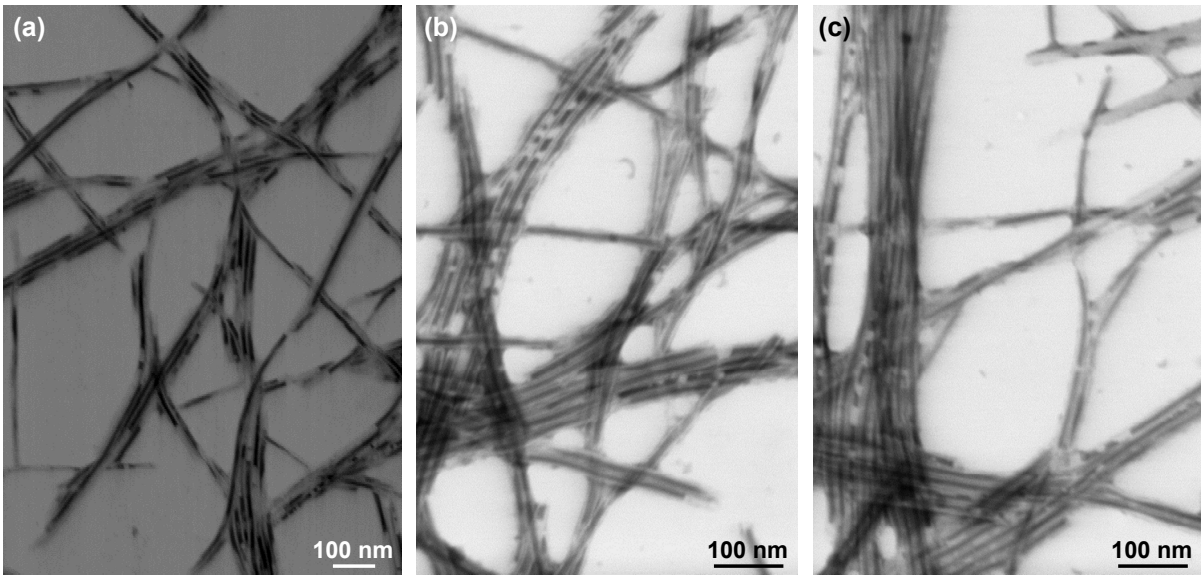

Fig. S1 (a) TEM image of the 2-nanotubes obtained by binary self-assembly of **1** and TGly in water. (b) TEM image of the GlcEG$_1$-nanotubes obtained by the heat treatment of the 2-nanotube with GlcEG$_1$. (c) TEM image of the GlcEG$_5$-nanotubes obtained by the heat treatment of the 2-nanotube with GlcEG$_5$. The hollow cylindrical space of the nanotubes is visible with phosphotungstate as a negative staining reagent.

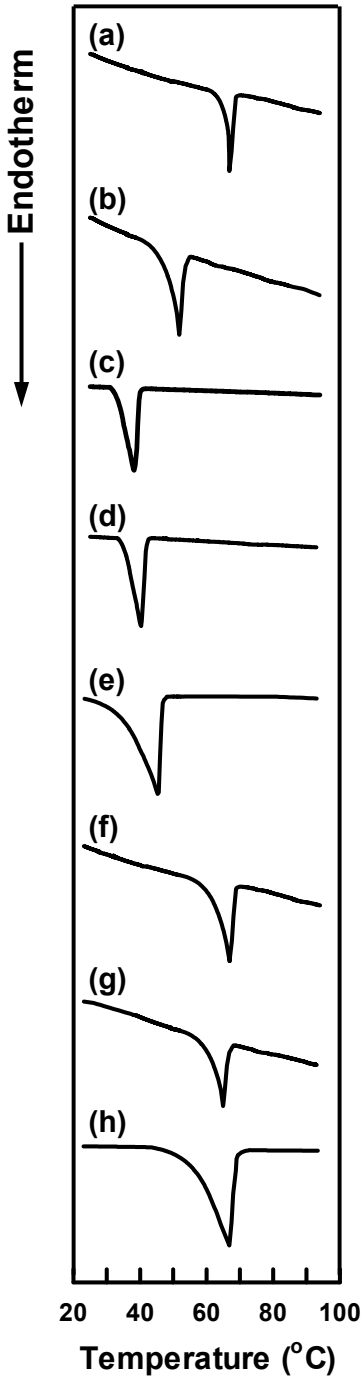

Fig. S2 DSC profiles of the fully hydrated self-assembled structures. Each nanostructure (1 mg) in the presence of water (20 mL) was placed in an aluminum pan to facilitate DSC measurements. (a) 1-nanotube formed by self-assembly of **1**, (b) 2-nanotube formed by binary self-assembly of **1** and TGly, (c) helical nanofiber formed by self-assembly of $GlcEG_1$, (d) helical nanofiber formed by self-assembly of $GlcEG_3$, (e) helical nanofiber formed by self-assembly of $GlcEG_5$, (f) $GlcEG_1$-nanotube formed by the heat treatment of the 2-nanotube with $GlcEG_1$, (g) $GlcEG_3$-nanotube formed by the heat treatment of the 2-nanotube with $GlcEG_3$, (h) $GlcEG_5$-nanotube formed by the heat treatment of the 2-nanotube with $GlcEG_5$.

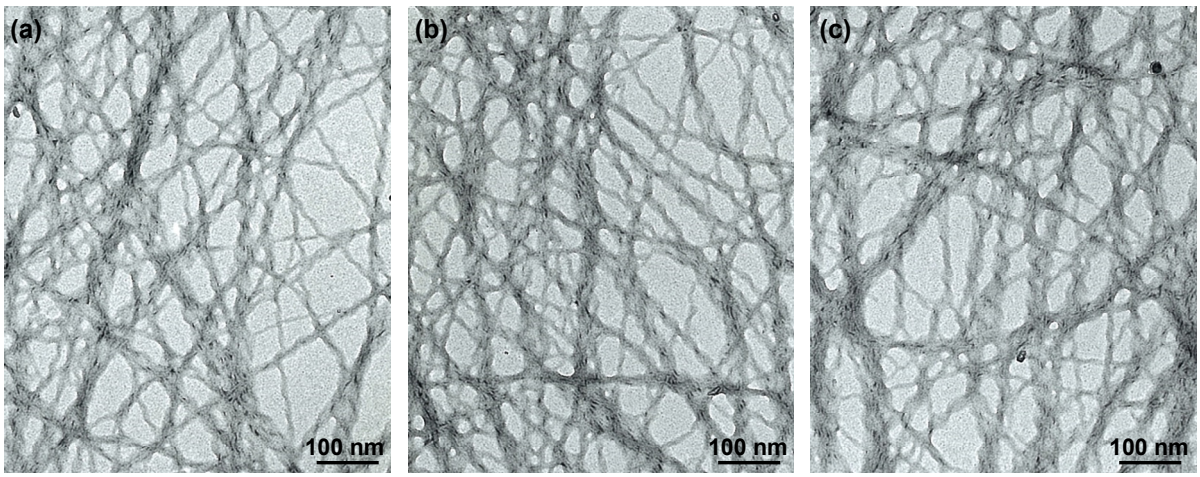

Fig. S3 (a) TEM image of the helical nanofibers obtained by self-assembly of $GlcEG_1$ in water. (b) TEM image of the helical nanofibers obtained by self-assembly of $GlcEG_3$ in water. (c) TEM image of the helical nanofibers obtained by self-assembly of $GlcEG_5$ in water.

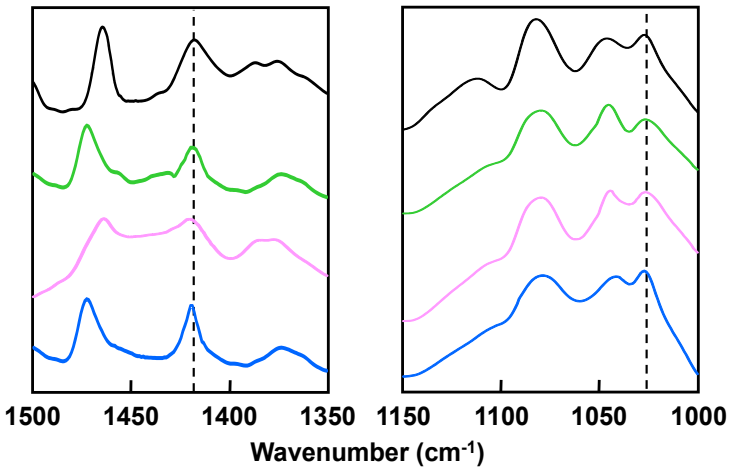

Fig. S4 The CH deformation (1420 cm^{-1}) and skeletal (1026 cm^{-1}) vibration bands for the triglycine moieties in the 1-nanotube (black line), $GlcEG_1$-nanotube (green line), $GlcEG_3$-nanotube (pink line), and $GlcEG_5$-nanotube (blue line).

Existence of those two bands suggests that TGly and the triglycine moiety of **1** forms polyglycine-II-type hydrogen bond network.*

* (a) T. Shimizu, M. Kogiso, M. Masuda, *J. Am. Chem. Soc.*, 1997, **119**, 6209; (b) C. H. Bamford, L. Brown, E. M. Cant, A. Elliott, W. E. Hanby, B. R. Malcolm, *Nature*, 1955, **176**, 396; (c) F. H. C. Crick, A. Rich, *Nature*, 1955, **176**, 780; (d) E.R. Blout, S. G. Linsley, *J. Am. Chem. Soc.*, 1952, **74**, 1946.

Table S1 IR absorption band of nanotubes

	1-nanotube	GlcEG$_1$-nanotube	GlcEG$_3$-nanotube	GlcEG$_5$-nanotube
Amide I / cm^{-1}	1642	1642	1644	1645
Amide II / cm^{-1}	1561	1561	1560	1560
δ(CH$_2$) / cm^{-1}	1465 (8.3)[1]	1465 (8.5)[1]	1465 (8.5)[1]	1465 (8.3)[1]
r(CH$_2$) / cm^{-1}	719	719	719	719

[1]Full width half-maximum

Single sharp peaks at 1465 and 719 cm^{-1} assignable to $\delta(CH_2)$ scissoring and $\gamma(CH_2)$ rocking vibration bands indicates that the lateral chain packing of the oligomethylene spacer in **1** and GlcEG$_n$ is of a triclinic parallel type.**

** a) N. Kameta, K. Ishikawa, M. Masuda, T. Shimizu, *Langmuir*, 2013, **23**, 13291; (b) N. Kameta, S. J. Lee, M. Masuda, *J. Mater. Chem. B*, 2013, **1**, 276; (c) N. Kameta, M. Masuda, H. Minamikawa, T. Shimizu, *Langmuir*, 2007, **23**, 4634; (d) N. Kameta, G. Mizuno, M. Masuda, H. Minamikawa, M. Kogiso, T. Shimizu, *Chem. Lett.*, 2007, **36**, 896.

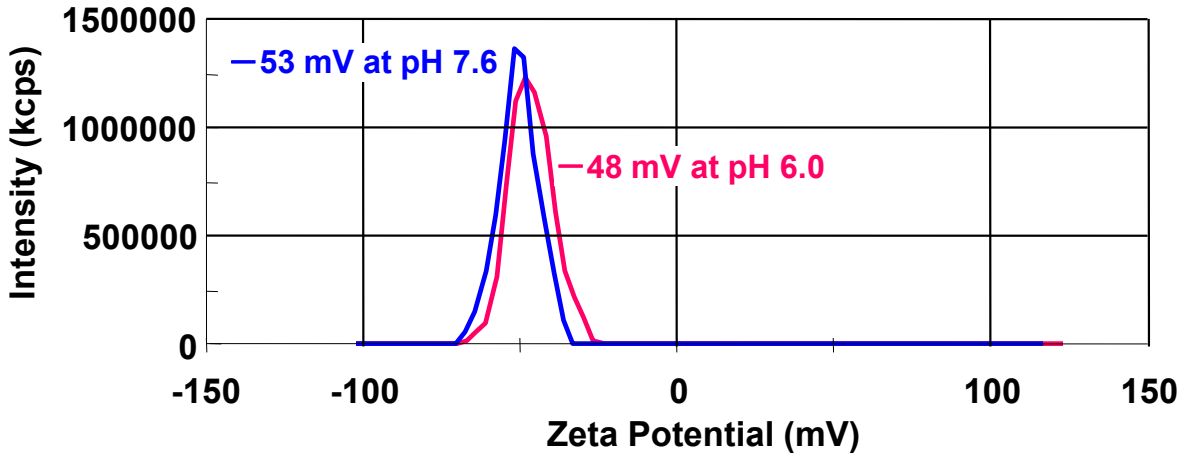

Fig. S5 The zeta potential distributions of the GlcEG$_3$-nanotube in water at pH 6.0 and 7.6. Each value was obtained from dynamic light scattering (DLS) measurements.

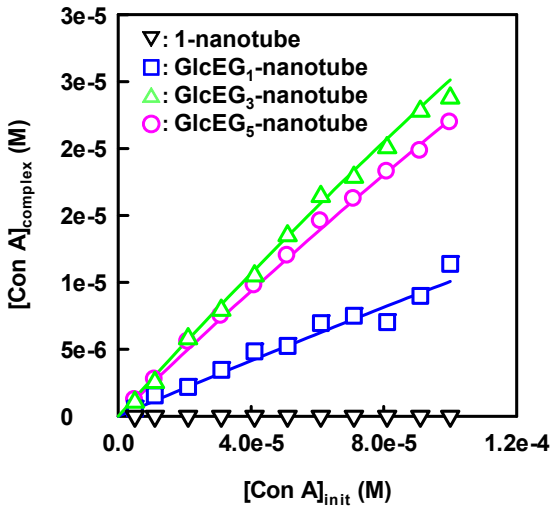

Fig. S6 Relationship between the initial concentration of Con A and the concentration of Con A complexed with the $GlcEG_n$-nanotubes. The latter concentration was estimated as the concentration of the isolated Con A with the $GlcEG_n$-nanotubes by filtration procedure, and was determined by UV/VIS spectroscopic measurements. The β values were determined by a nonlinear least squares fitting based on the general equation. Each solid line calculated by using β values is in good agreement with the experimental plots.

$$\beta = \frac{[GlcEG_n\text{-nanotube-Con A}]}{[GlcEG_n\text{-nanotube}][\text{Con A}]}$$

[Con A] was considered that Con A has four binding sites for the glucose moiety.

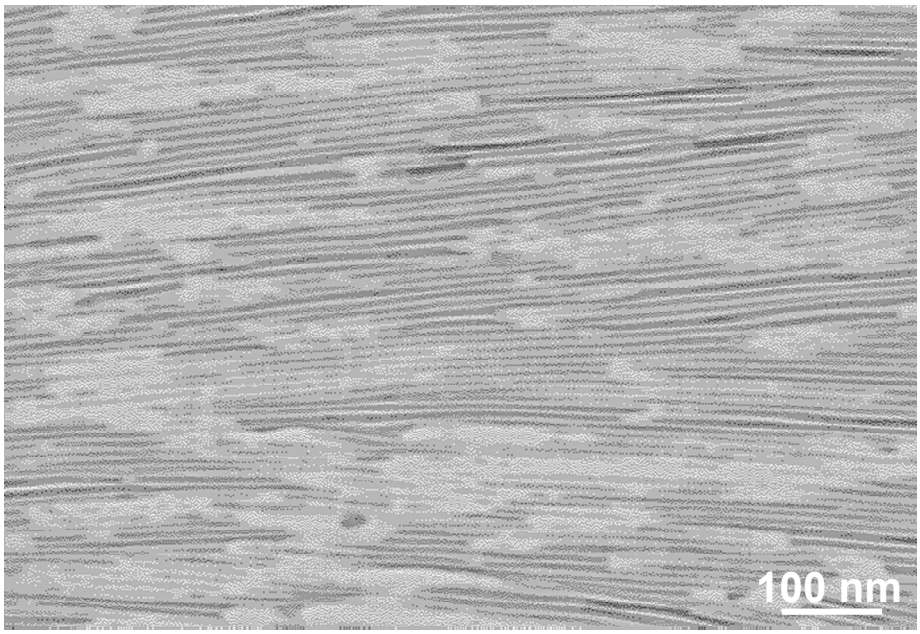

Fig. S7 TEM image of the liquid crystal in the dry state of $GlcEG_3$-nanotubes complexed with Con A. The hollow cylinder of the nanotubes can be visualized as dark contrasts with the negative staining reagent, 2wt% phosphotungstate.

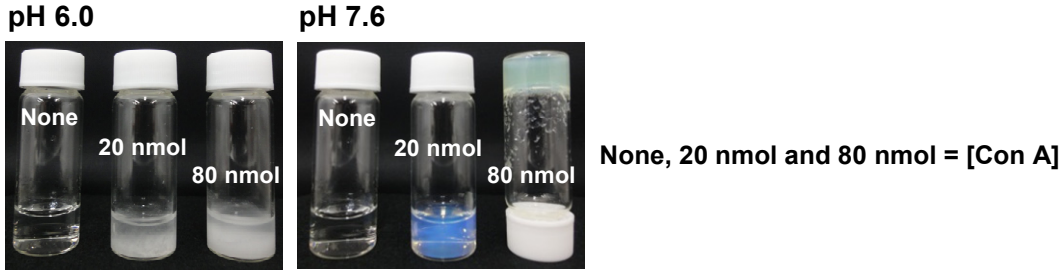

Fig. S8 Photographs of samples at pH 6.0 and 7.6 of the $GlcEG_3$-nanotube (1.1 mg/mL, **1** = 1.8 μmol, TGly = 0.2 μmol, $GlcEG_3$ = 0.2 μmol) in the presence and absence of Con A.

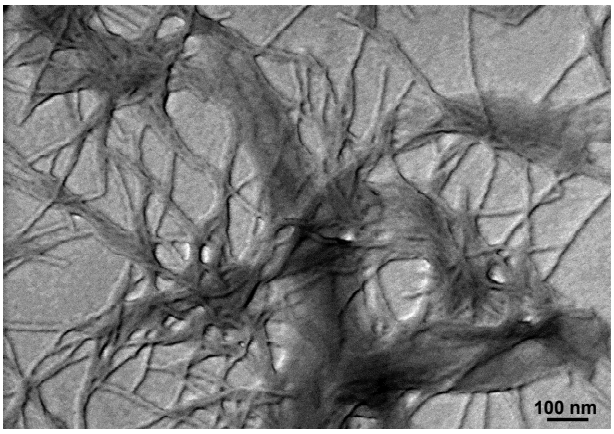

Fig. S9 SEM image of the $GlcEG_5$-nanotube dispersion in the presence of 20 nmol Con A.